Inflammasome assembly is required for intracellular formation of β2-microglobulin amyloid fibrils, leading to IL-1β secretion

Naoe Kaneko[1,§], Wakako Mori[2,§], Mie Kurata[1], Toshihiro Yamamoto[1], Tamotsu Zako[2]
and Junya Masumoto[1] ⊙

Abstract

Introduction: Dialysis-related amyloidosis (DRA) caused by β2-microgloblin (B2M) fibrils is a serious complication for patients with kidney failure on long-term dialysis. Deposition of B2M amyloid fibrils is thought to be due not only to serum extracellular B2M but also to infiltrating inflammatory cells, which may have an important role in B2M amyloid deposition in osteoarticular tissues in patients with DRA. Here, we asked whether B2M amyloid fibrils activate the inflammasome and contribute to formation and deposition of amyloid fibrils in cells.

Methods: Amyloid formation was confirmed by a thioflavin T (ThT) spectroscopic assay and scanning electron microscopy (SEM). Activation of inflammasomes was assessed by detecting interleukin (IL)-1β in culture supernatants from human embryonic kidney (HEK) 293T cells ectopically expressing inflammasome components. IL-1β secretion was measured by enzyme-linked immunosorbent assay. Expression and co-localization were analyzed by immunohistochemistry and dual immunofluorescence microscopy.

Results: B2M amyloid fibrils interacted directly with NLRP3/Pyrin and to activate the NLRP3/Pyrin inflammasomes, resulting in IL-1β secretion. When HEK293T cells were transfected with inflammasome components NLRP3 or Pyrin, along with ASC, pro-caspase-1, pro-IL-1β, and B2M, ThT fluorescence intensity increased. This was accompanied by IL-1β secretion, which increased in line with the amount of transfected B2M. In this case, morphological glowing of amyloid fibrils was observed by SEM. In the absence of ASC, there was no increase in ThT fluorescence intensity or IL-1β secretion, or any morphological glowing of amyloid fibrils. NLRP3 or Pyrin and B2M were co-localized in a "speck" in HEK293T cells, and co-expressed in infiltrated monocytes/macrophages in the osteoarticular synovial tissues in a patient with DRA.

Conclusion: Taken together, these data suggest that inflammasome assembly is required for the subsequent triggering of intracellular formation of B2M amyloid fibrils, which may contribute to osteoarticular deposition of B2M amyloid fibrils and inflammation in patients with DRA.

[1]Department of Pathology, Ehime University Graduate School of Medicine and Proteo-Science Center, Toon, Japan
[2]Department of Chemistry and Biology, Ehime University Graduate School of Science and Engineering, Matsuyama, Japan

§These authors contributed equally to this work

Corresponding author:
Junya Masumoto, Department of Pathology, Ehime University Graduate School of Medicine and Proteo-Science Center, Shitsukawa 454, Toon 791-0295, Japan.
Email: masumoto@m.ehime-u.ac.jp

Introduction

β2-microgloblin (B2M), a small subunit of human histocompatibility complex I, is located in the plasma membrane of cells within systemic tissues.[1] Dialysis-related amyloidosis (DRA) caused by B2M fibrils is a serious complication for patients with kidney failure long-term dialysis.[2,3] DRA is not limited to focal osteoarticular and synovial tissues such as the tenosynovium, which causes carpal tunnel syndrome, tendon sheaths, and the spine; it can occur in every organ. Clinical manifestations progress gradually, leading to a deterioration in quality of life.[4–7]

High local concentrations of B2M at an optimal pH of 2–3, or stabilization of B2M molecules, favor nucleation.[8] Although acidic conditions favorable to formation of B2M *in vivo* are not always physiological, B2M fibrils are deposited primally in osteoarticular tissues around the joints of DRA patients undergoing dialysis.[9] Systemic B2M amyloidosis was systemically observed in patients on long-term dialysis; these patients had chronic kidney failure and high serum B2M concentrations. Therefore, factors other than B2M accumulation seem to play a role in deposition of B2M in osteoarticular tissues.[10] Indeed, DRA is thought to be induced not only by B2M deposition but also by deposition of other biomolecules under favorable nucleation conditions.[11] Naiki *et al.*[12] established an *in vitro* nucleation-dependent polymerization model that explains the general mechanisms underlying amyloid fibril formation in various types of human and murine amyloidosis. Formation of amyloid fibers follows a classic nucleation-polymerization model in which a thermodynamically unfavorable nucleation reaction becomes favorable once a stable nucleus is formed.[11,12] Since deposition of B2M amyloid fibrils was not found in human B2M transgenic mice, even when injected with fibril seeds,[13] both serum extracellular B2M and infiltrating inflammatory cells could play an important role in B2M amyloid deposition in the osteoarticular tissues of patients with DRA. Indeed, high expression of B2M was found in lymphocytes, macrophages, and neutrophils that secrete IL-1β, and cellular production of IL-1 increased after hemodialysis.[14,15]

Previous studies indicated that amyloid-β (Aβ),[16] islets amyloid polypeptide (IAPP),[17] and serum amyloid A (SAA)[18,19] activate the nucleotide-binding oligomerization domain, a leucine-rich repeat and Pyrin domain containing (NLRP) 3 inflammasome. In addition, we reported that Aβ, IAPP, and insulin amyloid fibrils interact directly with NLRP3 and activate the NLRP3 inflammasome.[20–22] A recent report suggests that B2M acts as a driver that initiates inflammatory responses by myeloma-associated macrophages, the process of which depends on activation of the NLRP3 inflammasome after B2M accumulation in these cells.[23]

These facts prompted us to hypothesize that B2M amyloid fibrils interact directly with NLRP3 and activate the inflammasome, and that low intracellular concentrations of B2M amyloid fibrils activate the NLRP3 inflammasome, thereby triggering a chain reaction of B2M amyloid fibril formation.

In this study, we investigated whether B2M amyloid fibrils interact directly with NLRP3 and activate the intracellular NLRP3 inflammasome along the same pathway as Aβ, IAPP, and insulin amyloid fibrils. We also investigated whether intracellular B2M forms amyloid fibrils upon inflammasome activation to identify a possible additional role for inflammasome assembly in B2M amyloid fibril formation.

Methods

The nature of this study

The nature of this study is to investigate mechanism of B2M amyloidosis in view of protein chemistry and molecular basis of pathology. In order to achieve this purpose, experiments were conducted by the following methods.

Reagents

Recombinant human B2M was purchased from Wako (Oriental Yeast Co Ltd, Tokyo, Japan). Thioflavin T (ThT) was obtained from Sigma-Aldrich (St Louis, MO, USA).

Preparation of denatured monomeric B2M

B2M was dissolved in 2 M Gdn-HCl, 10 mM Tris-HCl buffer and 0.3 M NaCl (pH 8.5), and then was incubated for 1 h at 10°C to allow denaturation.[24,25] To remove the denaturation buffer, samples were placed in Slide-A-Lyzer Mini dialysis units (2000 MWCO, Thermo Scientific Pierce, Waltham, MA, USA) and dialyzed against 10 mM Tris-HCl containing 300 mM NaCl.

Formation of B2M amyloid fibrils

A solution containing 50 μM monomeric B2M was dissolved in 150 mM NaCl and 50 mM citrate acid (pH 3.0) as

described previously.[24,25] Formation of B2M fibrils was induced by incubating this solution at 70°C for 2 h without agitation.

Scanning electron microscopy

Protein samples (30 μg/mL) were dropped onto a silicon wafer and allowed to air-dry. Samples were observed under a field-emission-scanning electron microscopy (JSM7001FA, JEOL, Tokyo, Japan) at an acceleration voltage of 15 kV.

Thioflavin T spectroscopic assay

Protein samples (30 μg/mL) were mixed with a ThT solution (1 μM in PBS). Then, ThT fluorescence was measured using a microplate reader (BioTek Instruments, Winooski, VT, USA) at an excitation wavelength of 420 nm and an emission wavelength of 490 nm.

Plasmid construction

Plasmid pcDNA3-NLRP3-FLAG was constructed by inserting the complete NLRP3 coding sequence (CDS) into the BamH I and Xho I site of pcDNA3-FLAG. The NLRP3 CDS was derived from pDONR221-NLRP3.[26] pcDNA3-Pyrin-FLAG was constructed by inserting Pyrin CDS into the Kpn I and Xho I site of pcDNA3-FLAG. The Pyrin CDS was derived from pCMV4-FLAG-Pyrin.[27] The pcDNA3-apoptosis-associated speck-like protein containing a CARD (ASC) was constructed previously.[28] The pcDNA3-pro-caspase-1, pcDNA3-pro-interleukin (IL)-1β, and pcDNA3-B2M plasmids were constructed by inserting each CDS into the Kpn I and Xho I site of pcDNA3. The pro-caspase-1 CDS was derived from pDONR221-pro-caspase-1.[26] The pro-IL-1β CDS was derived from pDONR221-pro-IL-1β.[26] The B2M CDS was derived from a human EST clone (FLJ96890AAAF). pEU-E01-NLRP3-Biotin-ligation site (Bls) was constructed as previously described.[26] pEU-E01-nucleotide-binding oligomerization domain protein (NOD)2-Btn was constructed as previously described.[29] pEU-E01-Pyrin-Btn was constructed by inserting the Pyrin CDS into pEU-E01-GW-Bls. The Pyrin CDS which derived from pCMV4-FLAG-Pyrin was subcloned into pDONR221 using a two-step polymerase chain reaction (PCR). The first-step PCR product was amplified using the primers S1- Pyrin_F (CC ACC CACCACCACCAATGGCTAAGACCCCTAGTGACC) and Pyrin-T1(F)_R (TCCAGCACTAGCTCCAGAGTCAGGC-CCCTGACCACCCAC). The second step was carried out using the primers attB1-S1 (GGGGACAAGTTTGTA-CAAAAAAGCAGGCTTCCACCCACCACCACCAATG)

and attB2-T1 (GGGGACCACTTTGTACAAGAAAGCTG GGTCTCCAGCACTAGCTCCAGA). The second PCR product was inserted into a Gateway pDONR221 vector (Life Technologies, Carlsbad, CA, USA) using Gateway BP clonase II Enzyme mix (Life Technologies, Carlsbad, CA, USA) to generate entry clones. pDONR221-Pyrin was inserted into pEU-E01-GW-Bls for cell-free protein expression using Gateway LR clonase II Enzyme mix (Thermo Fisher Scientific, Waltham, MA, USA). These constructs were confirmed by sequencing. pEGFP-C2-NLRP3 was constructed by inserting the complete NLRP3 CDS into pEGFP-C2. The NLRP3 CDS was derived from pcDNA3-NLRP3-FLAG. pEGFP-C2-Pyrin was constructed by inserting the complete PYRIN CDS into pEGFP-C2. The Pyrin CDS was derived from pcDNA3-Pyrin-FLAG. pDsRed-Express2-C1-B2M was constructed by inserting the complete B2M CDS into pDsRed-Express2-C1. The B2M CDS was derived from pcDNA3-B2M-FLAG.

Recombinant protein synthesis

Cell-free protein expression of ASC and NLRP3 protein was reported previously.[26] The constructed plasmids were used to synthesize specific proteins with a WE-PRO1240 Expression Kit (Cell-free, Inc. Matsuyama, Japan), followed by Western blotting to confirm prompt protein synthesis.

Amplified luminescent proximity homogeneous assay

Synthesized protein–protein interactions were assessed using the amplified luminescent proximity homogeneous assay (ALPHA). The interaction between NLRP3 and B2M, Pyrin and B2M, or NOD2 and B2M was assessed. Pyrin-Btn or NOD2-Btn protein was synthesized by wheat germ protein synthesis system. Next, 1 μL of Pyrin-Btn, NLRP3-Btn, or NOD2-Btn were mixed with 1 μL of B2M in a 20 μL reaction premix. Finally, 10 μL of detection beads premix containing an anti-B2M mouse monoclonal antibody (sc-51,510: Santa Cruz Biotechnology, Inc. Dallas, TX, USA), streptavidin-conjugated alpha donor beads, and protein A/G conjugated alpha acceptor beads was mixed in the dark followed by incubation at 25°C for 24 h. The 1/2 area OptiPlate-96 was used for this assay. The final composition of the reaction mixture was 13 μM B2M, 0.1 M Tris-HCl (pH8.0), 0.01% (v/v) Tween 20, 1 mg/mL BSA, 0.05 μg/mL anti-B2M, 17 μg/mL streptavidin donor beads, and 17 μg/mL protein A/G acceptor beads. Fluorescence emission signals from each well were measured using an EnSpire™ Multimode Plate Reader (PerkinElmer, Waltham, MA, USA).

Reconstitution of the NLRP3 and Pyrin inflammasomes in human embryonic kidney 293T cells

Human embryonic kidney (HEK) 293T cells were maintained in DMEM (Thermo Scientific Gibco, Waltham, MA, USA) supplemented with 10% heat-inactivated FBS (Defined, endotoxin ≦ 10 EU/mL; Cytiva-HyClone Laboratories Inc. South Logan, UT, USA) and 100 U/mL penicillin-streptomycin (Thermo Scientific Gibco). Transfection was carried out using the calcium phosphate method.[30] HEK 293T cells (1×10^5) were co-transfected with the indicated amount of pcDNA3-NLRP3-FLAG or pEGFP-C2-NLRP3, pcDNA3-Pyrin-FLAG or pEGFP-C2-Pyrin, or pEGFP-C2 together with pcDNA3-ASC, pcDNA3-pro-caspase-1, and pcDNA3-pro-IL-1β (in triplicated wells). The indicated amounts of pcDNA3-B2M or pDsRed-Express2-C1-B2M were transfected in a dose dependent manner. The IL-1β concentration in the culture supernatants were measured using an enzyme-linked immunosorbent assay (ELISA) according to the manufacturer's instructions (BD Biosciences, San Jose, CA, USA).

Fluorescence microscopy for cellular localization

HEK293T cells were transfected with 300 ng of pEGFP-C2-NLRP3, pEGFP-C2-Pyrin, or pEGFP-C2, plus 300 ng of pDsRed-Express2-C1-B2M with or without 1 ng of pcDNA3-ASC, 10 ng of pcDNA3-pro-caspase-1, and 100 ng of pcDNA3-pro-IL-1β. After 24 h, green and red fluorescence signals were detected by immunofluorescence microscopy (BX-53, Olympus, Tokyo, Japan), and images were captured by a CCD camera (DP80, Olympus, Tokyo, Japan).

Immunohistochemical analysis

Hematoxylin and eosin staining and Congo-Red staining were carried out according to standard methods. Immunohistochemical analysis was carried out using the anti-NLRP3 mouse monoclonal antibody [Nalpy3-b], purchased from Enzo Life Sciences (Farmingdale, NY, USA) and used in our previous study.[31] An anti-β-2-microglobulin rabbit monoclonal antibody (D8P1H) was purchased from Cell Signaling Technology (Danvers, MA, USA). An anti-human CD68 mouse monoclonal antibody (PG-M1) was purchased from Dako (Carpinteria, CA, USA). Sections were obtained from formalin-fixed paraffin-embedded tissues. The sections (3 μM thick) were deparaffinized in xylene and rehydrated through a decreasing concentration of ethanol solutions. For bright field histochemistry, endogenous peroxidase activity was blocked by addition of 0.3% H_2O_2 in methanol for 30 min. Before immunostaining, antigen retrieval was carried out by incubating tissue sections in a microwave in 10 mmol/L Tris-HCl buffer (pH 8.0) containing 1 mmol/L ethylenediaminetetraacetic acid (EDTA). Sections were blocked with 1% normal bovine serum in 50 mmol/L Tris-buffered saline (TBS) (pH 7.6) and incubated overnight at 4°C with primary antibodies diluted in blocking buffer. Binding was detected using EnVision+ mouse or rabbit/HRP (Dako, Carpinteria, CA, USA), and positive signals were revealed by the addition of diaminobenzidine tetrahydrochloride (DAB) for bright field immunohistochemistry, or Alexa Fluor 488 and Alexa Fluor 647 AffiniPure F (ab)$_2$ fragment goat anti-mouse IgG (H + L) (Jackson ImmunoResearch, West Grove, PA, USA) for immunofluorescence microscopy and dual immunofluorescence analysis. Tissue sections used for bright field immunohistochemistry were counterstained with hematoxylin and mounted in Entellan new (Sigma-Aldrich, St Louis, MO, USA). Tissue sections used for immunofluorescence microscopy were mounted in ProLong Glass Antifade Mountant with NucBlue (Hoechst 33,342) (Life Technologies, Eugene, OR, USA). A control experiment was performed by omitting the primary antibody from the staining procedure.

Clinical samples

Paraffin-embedded blocks of osteoarticular tissue from patients with DRA were selected from the pathology files of the Department of Pathology of Ehime University. The study was approved by the Human Research Ethical Committee of Ehime University (reference number 1301001).

Thioflavin T staining

Deparaffinized section was counter-stained with hematoxylin for 1 min and stained for 3 min with 1% ThT filtrated by 0.45-μm pore-filter. Then the section was differentiated for 1 min in 1% aqueous acetic acid.

Statistical analysis

All results are presented as the mean ± standard deviation of triplicate wells, and the significance of differences was evaluated using the Mann–Whitney U test. A p-value <0.05 was considered significant.

Results

B2M amyloid fibrils interact directly with both NLRP3 and Pyrin

First, we tested whether B2M amyloid fibrils interact directly with NLRP3 in our cell-free system. Formation of amyloid fibrils was confirmed by the ThT assay and by SEM analysis (Figure 1(a) and (b)). As shown in the figure,
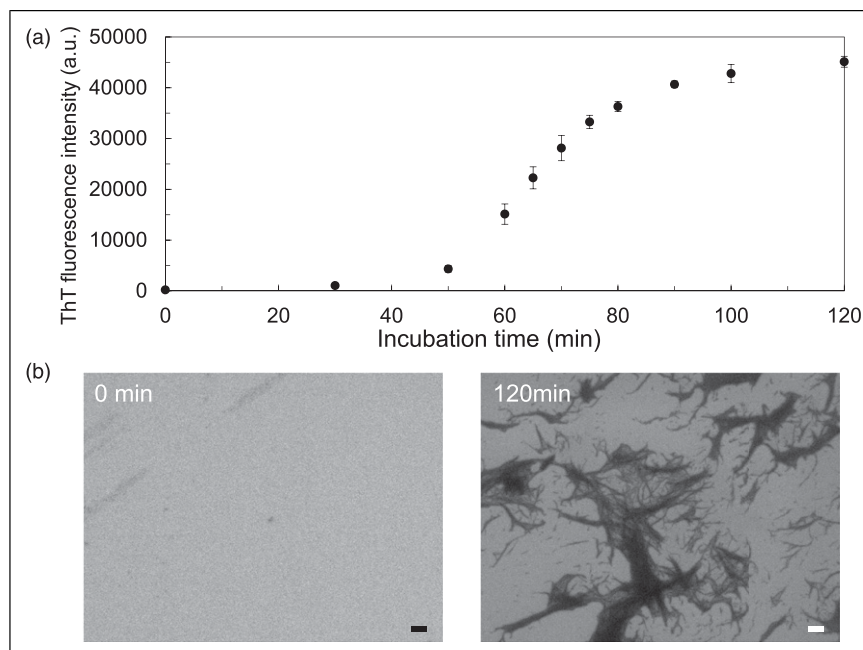
Figure 1. Formation of B2M amyloid fibrils and morphological changes. **(a)** Time course of the ThT assay revealed showing formation of B2M amyloid fibrils under oligomerization conditions for 120 min at 70°C. **(b)** Morphological images of B2M under oligomerization conditions for 0 min (left panel) and 120 min (right panel) at 70°C. Scale bars 1 μm. Data are representative of two independent experiments.

formation of B2M amyloid fibrils was confirmed after a 120-min incubation with 50 μM B2M at pH3.0, which is consistent with the previous study.[25] Another previous study shows that the structure of the amyloid fibrils formed at acidic pH is similar to that formed at neutral pH.[32] Figure 2(a) shows schematics of the C-terminal biotinylated full-length NOD2 (NOD2-Btn), NLRP3 (NLRP3-Btn), Pyrin (Pyrin-Btn), and non-tagged B2M used in the experiments (Figure 2(a)). ALPHA signals emitted between NLRP3-FLAG, or Pyrin-FLAG and B2M amyloid fibrils were higher than those emitted by an unbounded control between NOD2 and B2M (Figure 2(b)). Next, we performed immunoprecipitation followed by Western blot analysis to further confirm the interactions between B2M amyloid fibrils and NLRP3 or Pyrin. The immunoprecipitation experiment was performed as described previously.[33] Consistent with the ALPHA experiments, we found that non-tagged B2M amyloid fibrils co-immunoprecipitated with NLRP3-FLAG or Pyrin-FLAG, but not with NOD2-FLAG (an unbound negative control) (Figure 2(c)).

B2M alone does not form amyloid fibrils in living cells

To investigate whether B2M forms amyloid fibrils in living cells, we transfected HEK293T cells with pcDNA3-B2M. Briefly, HEK293T cells (in triplicate cells) were transfected with 0, 10, 100, or 1000 ng non-tagged pcDNA3-B2M for 24 h. Each cell lysate was subjected to a ThT assay. There was no significant increase in ThT fluorescence intensity at any of the concentrations used (Figure 3(a)).

ASC is required for assembly of the inflammasome and for intracellular formation of B2M amyloid fibrils, resulting in secretion of IL-1β by HEK293T cells

We reconstituted the NLRP3 and Pyrin inflammasome in HEK293T cells to investigate whether they were activated by B2M. HEK293T cells were transfected with the indicated amounts of pcDNA3-NLRP3-FLAG, pcDNA3-Pyrin-FLAG, or pEGFP-C2, plus pcDNA3-ASC, pcDNA3-pro-caspase-1, and pcDNA3-pro-IL-1β together with the indicated amounts of pcDNA3-B2M (Figure 3(b)). The ThT assay revealed a significant increase in ThT fluorescence intensity in HEK293T cells reconstituted with the NLRP3 and Pyrin inflammasomes and transfected with B2M (Figure 3(b)). Notably, the ThT fluorescence intensity of HEK293T cells reconstituted with the NLRP3 or Pyrin inflammasome in the absence of pcDNA3-ASC and transfected with pcDNA3-B2M was significantly lower than that of cells transfected with pcDNA3-ASC (Figure 3(b)). ThT fluorescence intensity, a measure of amyloid fibril formations, showed a relationship with IL-1β
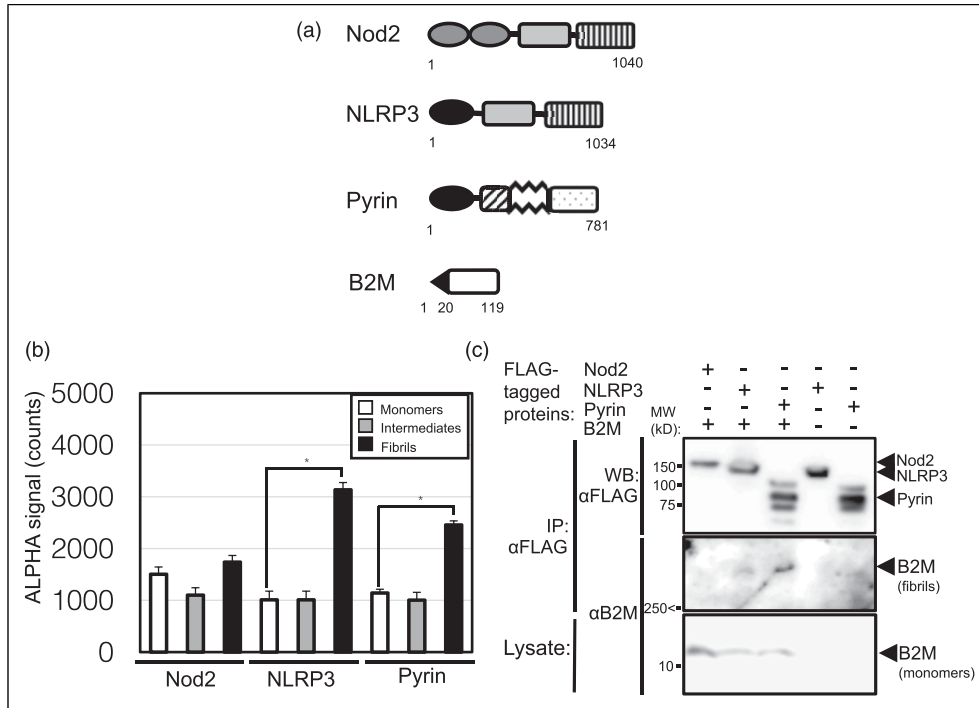
Figure 2. B2M amyloid fibrils interact with NLRP3 and Pyrin. **(a)** Schematic representations of NOD2, NLRP3, Pyrin, and B2M. The PYRIN domain (PYD) is indicated by black boxes. The caspase recruitment domain (CARD) is indicated by a dark gray box. The nucleotide-binding oligomerization domain (NOD) is indicated by a light gray box. Leucine-rich repeats (LRRs) are indicated by a striped box. The zinc finger domain (b-Box), a coiled coil (CC) domain and a B30.2/SPRY domain in Pyrin are indicated by a hatched box, a jagged box, and a punctate box, respectively. The black triangle in B2M indicates a signal peptide. Amino acid sequence numbers are indicated under each schema. **(b)** Synthetic protein–protein interactions between C-terminal Biotinylated NOD2, NLRP3, or Pyrin and B2M were assessed in an amplified luminescent proximity homogeneous assay. Results are expressed as the mean ± standard deviation. *A p-value < .05 was considered significant. Data are representative of three independent experiments. **(c)** Interaction between NLRP3-FLAG or Pyrin-FLAG and B2M was assessed by immunoprecipitation. NOD2 was used as a negative control for immunoprecipitation as it is representative of other NOD-like receptors. IP, immunoprecipitation; WB, Western blot analysis; Lysate, lysate before immunoprecipitation.

secretions (Figure 3(c)). Next, we examined morphological changes using SEM (Figure 4). Consistent with the data of the ThT (Figure 2(b)), morphological changes were observed in lysates of HEK293T cells reconstituted with NLRP3 or Pyrin (but not EGFP) inflammasome and transfected with 10 ng or 50 ng pcDNA3-B2M (Figures 4(a)–(c)). Notably, and consistent with ThT assay results (Figure 2(b)), HEK293T cells transfected with 50 ng of pcDNA3-B2M in the absence of ASC showed no amyloid fibril in SEM (Figure 4(a) and (b)).

We further confirmed the intracellular co-localization between B2M and NLRP3 or Pyrin in HEK293T cells by fluorescence microscopy (Figure 5). HEK293T cells were transfected with pEGFP-C2-NLRP3, pEGFP-C2-Pyrin, or pEGFP-C2, plus pcDNA3-ASC, pcDNA3-pro-caspase-1, and pcDNA3-pro-IL-1β together with pDsRed-Express2-C1-B2M (Figure 5). Consistent with the results presented in Figure 4, NLRP3 (green) and B2M (red) accumulated in the same speck-like aggregate when co-expressed with

inflammasome components (Figure 5). Notably, both NLRP3 and B2M co-localized diffusely in the cytoplasm in the absence of ASC or any of the inflammasome components (Figure 5). Pyrin (green) and B2M (red) accumulated in the same speck-like aggregate when co-expressed with inflammasome components, as well as NLRP3 (Figure 5). Both Pyrin and B2M co-localized diffusely in the cytoplasm in the absence of ASC or any of the inflammasome components. Differential interference contrast image (DIC) revealed that HEK 293T cells were viable (Figure 5).

NLRP3 and B2M co-localized in monocytes/macrophages infiltrating the osteoarticular synovial tissues in a patient with DRA

Next, we performed immunohistochemical analysis to confirm whether monocytes/macrophages expressing NLRP3 infiltrated the osteoarticular synovial tissue in a
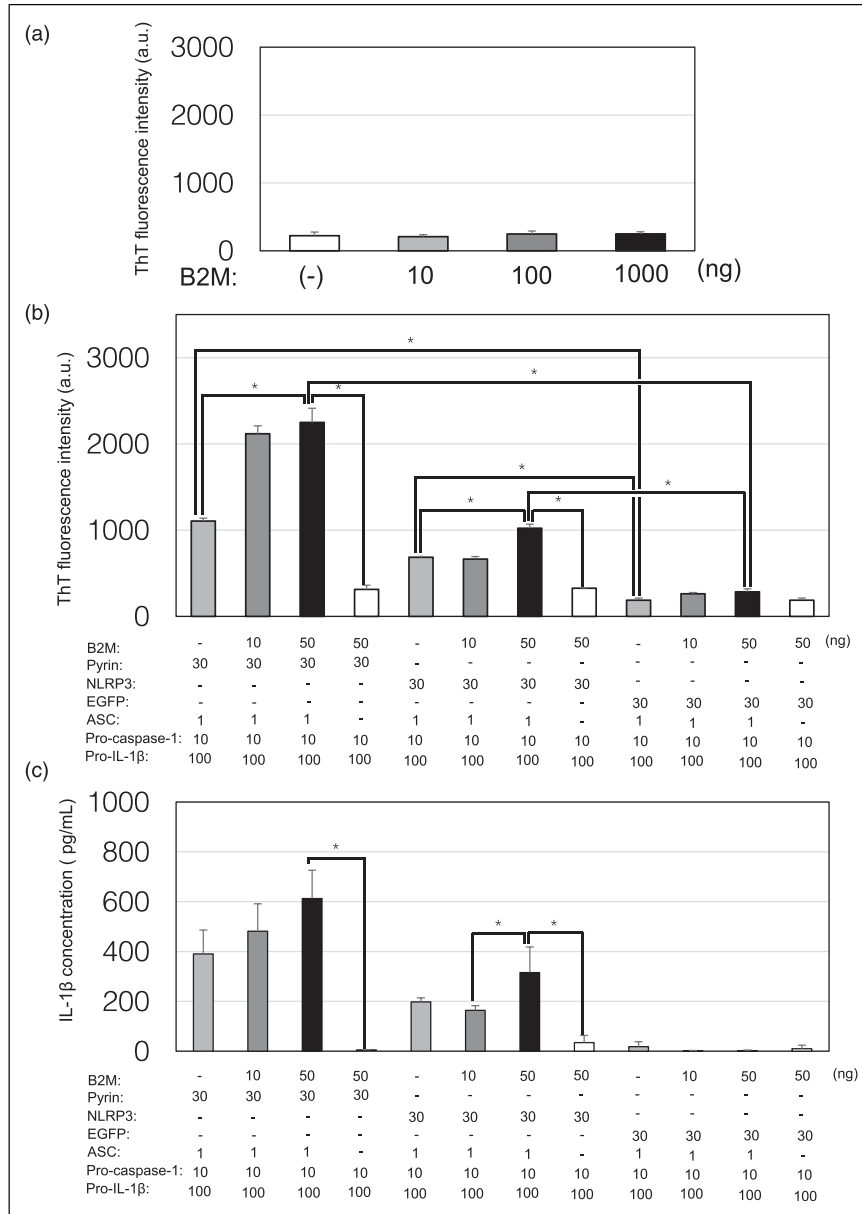
Figure 3. ASC is required for formation of amyloid fibrils and inflammasome activation. **(a)** ThT assay of lysates derived from HEK293T cells transfected with the indicated amounts (in triplicate wells) of pcDNA3-B2M revealed formation of B2M amyloid fibrils. **(b)** ThT assay of lysates derived from HEK293T cells transfected with the indicated amounts (in triplicate wells) of each indicated plasmid. *A p-value <0.05 was considered significant. **(c)** IL-1β concentration in the culture supernatant of HEK293T cells transfected with the indicated amounts (in triplicate wells) of each indicated plasmid. *A p-value < .05 was considered significant.

patient with DRA. Extreme amyloid deposition was observed by hematoxylin and eosin, Congo-Red, and ThT staining (Figure 6(a)–(d)). NLRP3 was detected in infiltrating cells that were morphologically consistent with monocytes/macrophages (Figure6(e) and (f)). These cells were positive for CD68, a monocytes/macrophages marker (Figure 6(g) and (h)). B2M was detected in deposited materials, and in infiltrating monocytes/macrophages around the deposited amyloid (Figure 6(i) and (j)). There was no non-specific staining of the negative controls (Figure 6(k) and (l)).

We used immunofluorescence microscopy to confirm whether NLRP3 and B2M co-localized in the same field (Figure 7). The green fluorescence signals (NLRP3) and
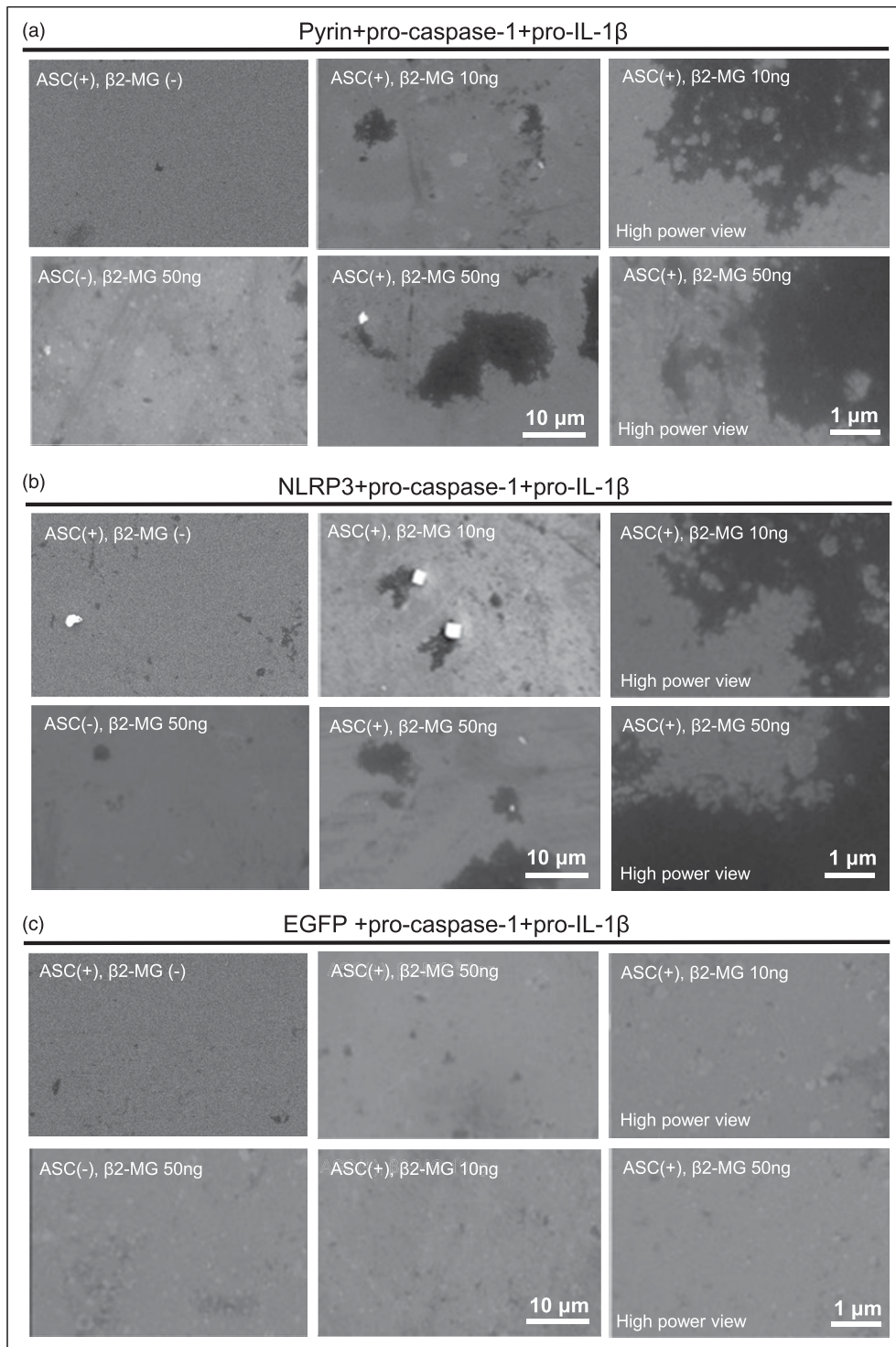
Figure 4. Morphological images of the corresponding lysate examined in Figure 3(b). Morphological changes were noted. **(a)** Pyrin-FLAG, pro-caspase-1, pro-IL-1β, and B2M with or without ASC were expressed in HEK293T cells. **(b)** NLRP3-FLAG, pro-caspase-1, pro-IL-1β, and B2M with or without ASC were expressed in HEK293T cells. **(c)** EGFP, pro-caspase-1, pro-IL-1β, and B2M with or without ASC were expressed in HEK293T cells. Scale bars, 10 μm and 1 μm (high power view).
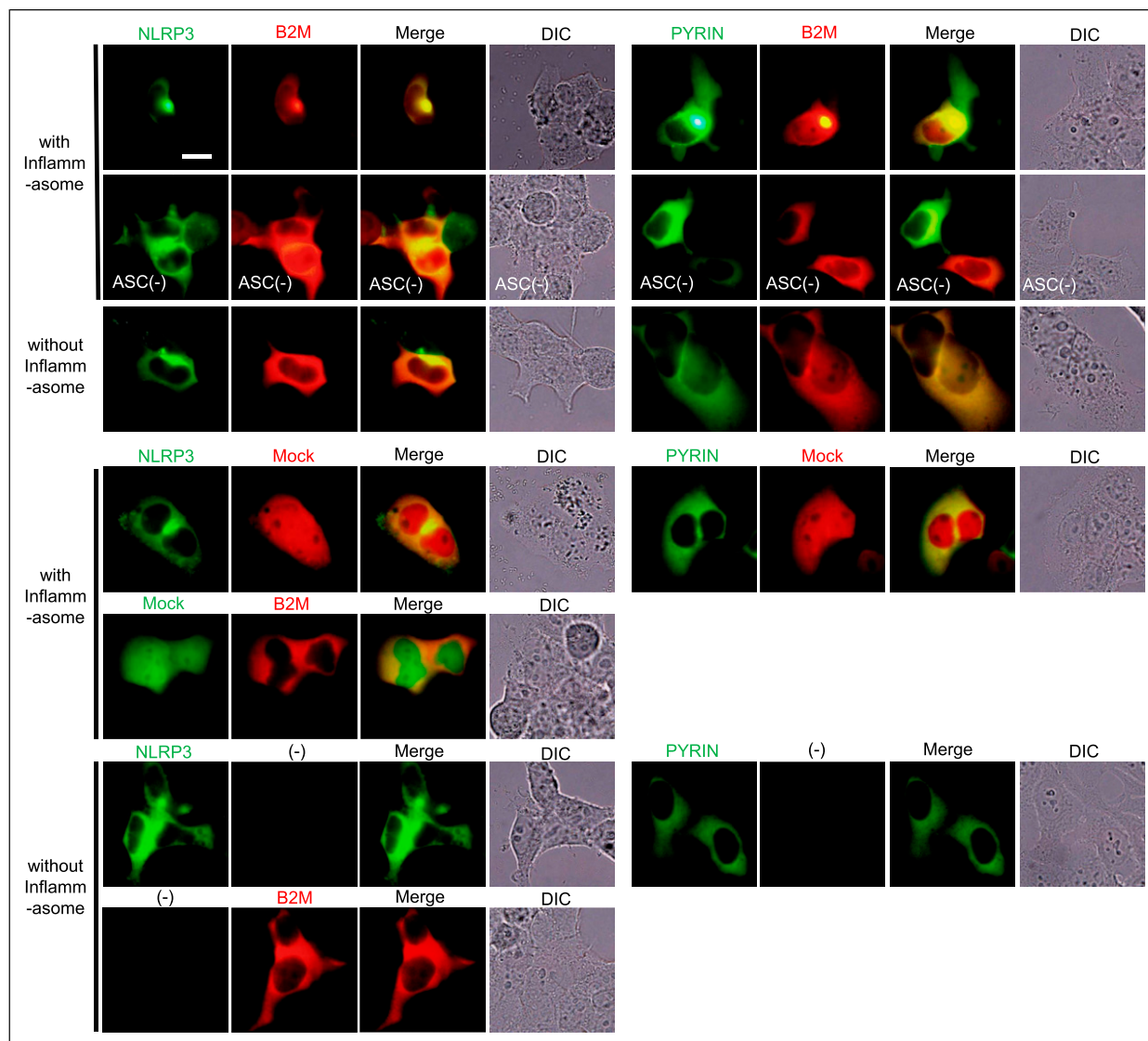
Figure 5. Fluorescence microscopy analysis of cellular localization. HEK293T cells ectopically expressing EGFP-NLRP3, EGFP-Pyrin, or EGFP-Mock, plus DsRed-B2M with or without ASC, pro-caspase-1, and pro-IL-1β. Green and red fluorescence signals were detected under an immunofluorescence microscope. Merged images of green and red fluorescence are also presented. Differential interference contrast image (DIC) of the same filed. Scale bar, 20 μm.

the red fluorescence signals (B2M) were merged in infiltrating cells, which were morphologically identical to monocytes/macrophages (Figure 7, arrowheads) Nuclear staining of blue (Hoechst 33,342), green (NLRP3), red (B2M) and merged images suggested that B2M was both inside and outside of a cell, and deposited in the osteoarticular tissues in a patient with DRA, and green fluorescence signals (NLRP3) were accumulated in a "speck" with red fluorescence signals in a pyroptotic cell, having no nuclear blue fluorescence signal (B2M) (Figure 7, arrows). DIC and DIC plus merged images revealed that infiltrating monocytes/macrophages were around B2M

amyloid deposition of the osteoarticular tissues in a patient with DRA.

Discussion

DRA characterized by focal accumulation and systemic tissue deposition of amyloid fibrils is a serious complication of long-term dialysis.[34] DRA can lead to life-threatening clinical manifestations such as destructive spondyloarthropathy, fractures, gastrointestinal involvement, and cardiovascular amyloidosis.[7] Therefore, development of attractive therapeutic targets and
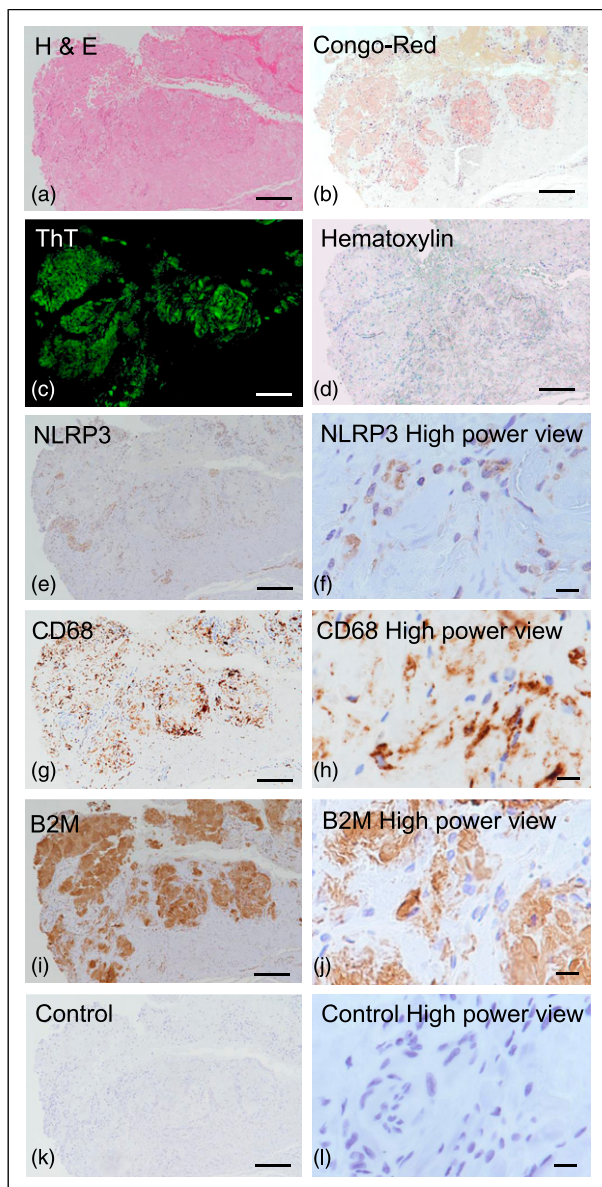
Figure 6. Expression of NLRP3 and B2M in osteoarticular tissue. Formalin-fixed and paraffin-embedded specimens from a patient with dialysis-related amyloidosis were stained with hematoxylin and eosin (H and E) **(a)**, Congo-Red **(b)**, and ThT **(c)** with hematoxylin counter stain **(d)**. Serial sections were immunostained with antibodies specific for NLRP3 **(e and f)**, CD68 **(g and h)** and B2M **(i and j)**. A negative control (lacking the primary antibody) is also included **(k and l)**. Scale bars, 200 μm.and 20 μm (high power view).

Figure 7. Dual immunofluorescence staining of NLRP3 and B2M in osteoarticular tissue. Green NLRP3 fluorescence and red B2M fluorescence signals were detected. Nuclear blue Hoechst 33342 signals were also detected. Merged images show green (NLRP3), red (B2M), and blue (Hoechst 33342) fluorescence. Differential interference contrast image (DIC) and DIC plus merged images of the same filed were shown. Scale bar, 10 μm.

therapies is awaited. The amyloid fibrils, isolated from a chronic hemodialysis patients, were identified as B2M.[9]

Previous studies showed that nucleation-polymerization is required for formation of B2M amyloid fibrils under acidic conditions (pH of 2–3).[35] Consistent with this, we found that B2M formed amyloid fibrils at low (pH3) pH and high (50 μM) concentrations (Figure 1(a) and (b));

however, low pH conditions are not common in human body. Formation of B2M amyloid fibrils may be supported by other molecules such as ApoE, proteoglycans, glycosaminoglycans, type-1 collagen, non-esterified fatty acids, and lysophospholipids.[36,37] Thus, factors other than β2M accumulation also seem to play a role in the deposition of B2M in osteoarticular tissues. Then, we hypothesized that intracellular low concentration of B2M amyloid fibrils can directly activate NLRP3 inflammasome, leading to trigger chain reaction of formation of B2M amyloid fibrils. Since inflammasome activation is known to induce pyroptotic cell death accompanied by IL-1β secretion, intracellular B2M amyloid fibrils may secrete and deposit extracellular matrix with IL-1β secretion which may induce further inflammation.

Because we reported previously that IAPP, Aβ, and insulin amyloid fibrils interact directly with the NLRP3 inflammasome,[20–22] we thought that B2M might also interact with NLRP3 to support formation of amyloid fibrils. As expected, we observed a high ALPHA signal for NLRP3-Btn plus B2M amyloid fibrils (Figure 2(b)). In addition, we also observed a high ALPHA signal for Pyrin-

Btn plus B2M amyloid fibrils (Figure 2(b)), suggesting that B2M amyloid fibrils interacts with NLRP3 and Pyrin. This was surprising because we selected Pyrin and NOD2 as comparable negative controls for NLRP3. Therefore, we performed immunoprecipitation followed by western blotting to confirm the above results. Consistent with the ALPHA experiments, non-tagged B2M amyloid fibrils co-immunoprecipitated with NLRP3-FLAG or Pyrin-FLAG but not with NOD2-FLAG (Figure 2(c)), suggesting that both NLRP3 and Pyrin form a complex with B2M amyloid fibrils.

A previous study pointed out that B2M is located in granules in neutrophils and monocytes.[38] The proteases in azurophilic granules of neutrophils and monocytes infiltrated into the synovial fluid plays an important role in formation of amyloid fibrils.[39] Also Pyrin and NLRP3 are expressed in neutrophils and monocytes.[40] Thus, we hypothesized that inflammasome formation may contribute to intracellular formation of B2M amyloid fibrils and the intracellular formation of B2M amyloid fibrils could contribute to amyloid deposition in osteoarticular tissues in patients with DRA.

Then, we used a reconstituted inflammasome in HEK293T cells to test whether B2M forms fibrils with the NLRP3 and Pyrin inflammasome. HEK293T cells are one of the most widely used cell lines for biological research into signal transduction, cancer, and protein expression.[41] In addition, reconstruction of the inflammasome in HEK293T cells is widely accepted in the field of inflammasome research because HEK293T cells do not spontaneously secrete IL-1β.[42,43] Thus, we reconstituted the NLRP3 inflammasome in HEK293T cells for the cell-based inflammasome-activating assay for B2M.

Expression of B2M protein alone in HEK293T cells yielded no significant ThT fluorescence intensity (Figure 3(a)). These data seem reasonable because the concentration of expressed B2M was lower than cell-free condition. Low solubility, agitation, or seeding is thought to be required for formation of amyloid fibrils.[44,45] When Pyrin or NLRP3, along with pro-caspase-1, pro-IL-1β, and ASC, was expressed ectopically in HEK293T cells, we observed high ThT fluorescence intensity in cells that were also transfected with B2M (Figure 3(b)). Notably, ThT fluorescence intensity and IL-1β secretion from HEK293T cells reconstituted with the NLRP3 or Pyrin inflammasome increased; however, secretion in the absence of ASC was much lower than in the presence of ASC (Figure 3(b) and (c)), suggesting that ASC is crucial for formation of amyloid fibrils and for IL-1β secretion. Figure 4 shows that morphological formation of fibrils is consistent with the results of the ThT assay (Figure 3(b)). Because EGFP could not form an inflammasome, even when ASC was present, formation of amyloid fibrils or secretion of IL-1β was not observed (Figure 3(c)). Therefore, the data suggests that

formation of an inflammasome in the presence of ASC triggers formation of B2M amyloid fibrils and secretion of IL-1β. Indeed, cellular IL-1 production increases after hemodialysis.[14,15] These data partially support a role for ASC plus Pyrin in AA-type amyloid deposition in patients with familial Mediterranean fever.[46]

Next, to clarify intracellular or extracellular interaction between B2M and NLRP3 or Pyrin in HEK293T cells, we performed fluorescence microscopy analysis after ectopic expression of EGFP-tagged NLRP3 and DsRed-tagged B2M, with or without ASC or inflammasome components (Figure 5). Consistent with the results presented in Figure 4, NLRP3 (green) and B2M (red) accumulated in the same "speck" when co-expressed with inflammasome components (Figure 5). Notably, both NLRP3 and B2M co-localized diffusely in the cytoplasm in the absence of ASC or all inflammasome components (Figure 5). Pyrin (green) and B2M (red) also accumulated in the same speck-like aggregate when co-expressed with inflammasome components and NLRP3 (Figure 5). Both Pyrin and B2M were co-localized diffusely in the cytoplasm in the absence of ASC or all inflammasome components (Figure 5). Since ASC is indispensable for inflammasome formation, these data suggest that inflammasome formation may be required for formation of B2M amyloid fibrils and not only for the interaction between B2M and Pyrin or NLRP3.

To obtain pathologically relevant data, we performed immunohistochemical studies in tissue from a patient with DRA (Figure 6). NLRP3 was detected in CD68-positive infiltrating monocytes/macrophages in a ThT-positive amyloid-deposited osteoarticular tissue in a patient with DRA (Figure 6(a)–(h)) and was partially co-expressed with B2M, which was also detected in deposited materials (Figure 6(i) and (j)). We further confirmed whether NLRP3 and B2M co-localized in the same field using dual immunofluorescence microscopy. The green fluorescence signals (NLRP3) co-localized with the red fluorescence signals (B2M) in infiltrating cells, which were morphologically identical to monocytes/macrophages. B2M exist inside and outside of cells, and deposited around the infiltrating monocytes/macrophages (Figure 7). These data provide physiologically relevant evidence to support our hypothesis and suggest that intracellular B2M amyloid can be released and deposited from monocytes/macrophages in the extracellular matrix, where it plays a role in extracellular amyloid formation (Figure 7 and 8).

Although the results were highly reproducible, there are several limitations due to our use of a cell-free system and a reconstituted inflammasome in HEK293T cells. First, the efficient B2M amyloid formation was observed only under the acidic conditions described for the cell-free system. Importantly, the structure of amyloid fibrils formed at acidic pH is similar to that formed at pH 7.0.[32] In addition,
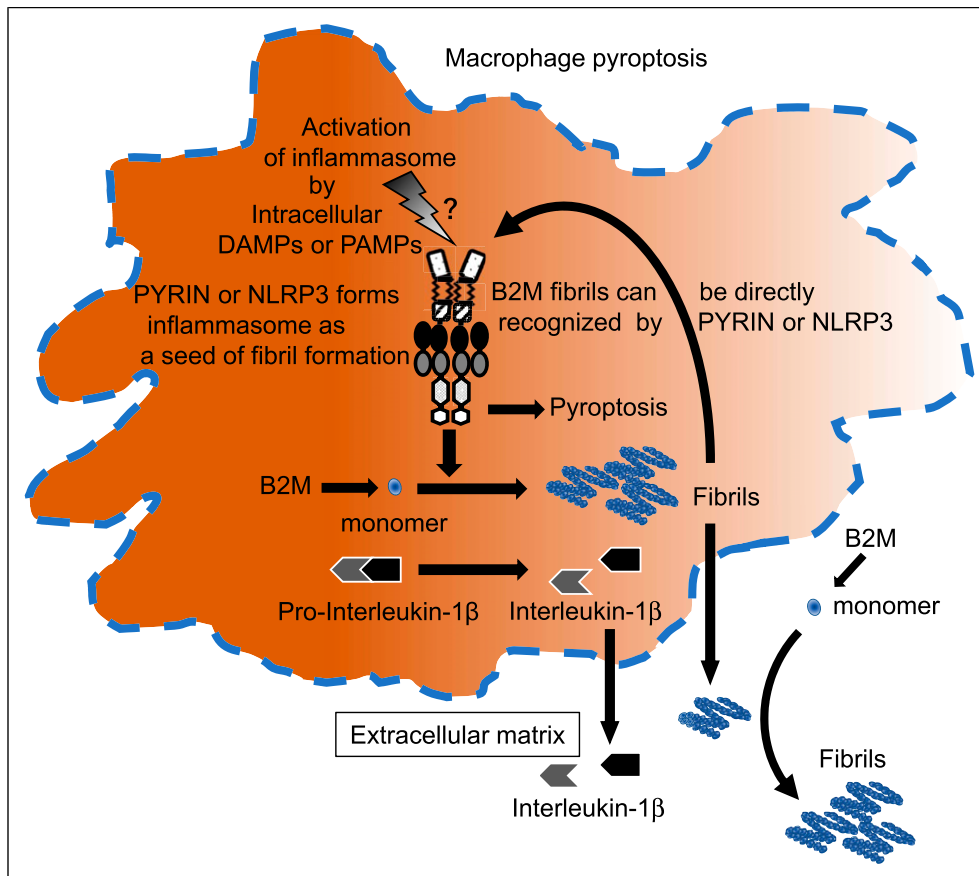
Figure 8. Inflammasome assembly is required for subsequent triggering of intracellular B2M amyloid fibril formation. Intracellular DAMPs/PAMPs activate the inflammasome, which acts as a seed for formation of amyloid fibrils by infiltrating macrophages in osteoarticular tissue, accompanied by Il-1β secretion and pyroptotic cell death (pyroptosis).

Hofbauer et al.[23] recently reported that internalized B2M phagocytosed by macrophages aggregates into amyloid fibrils under acidic phagosomal conditions and then activates the NLRP3 inflammasome. Although we know that acidic conditions are not always physiological, the B2M fibrils formed under highly acidic conditions may not be the same as those formed under physiological conditions.

Second, we used a reconstituted inflammasome in HEK293T cells, rather than neutrophils or monocytes, as a model of intracellular B2M amyloid fibril formation in living cells. HEK293T cells are one of the most widely used cell lines for biological research.[41] In addition, reconstruction of the inflammasome system in HEK293T cells is widely accepted in the field because these cells do not spontaneously secrete IL-1β.[42] Although ectopic expression of B2M amyloid fibrils was observed in HEK293T cells with a reconstituted inflammasome, this does not perfectly reflect B2M amyloid deposition in osteoarticular tissues in DRA. Therefore, we performed an immunohistochemical study using anti-human NLRP3 and B2M antibodies in human patients' tissues and found that both accumulated in osteoarticular lesions (Figure 7).

Conclusions

B2M amyloid fibrils interacted directly with NLRP3/Pyrin to activate the NLRP3/Pyrin inflammasomes, resulting in IL-1β secretion. ASC is required for assembly of inflammasomes and for intracellular formation of B2M amyloid fibrils; therefore, inflammasome assembly is required for the subsequent triggering of intracellular formation of B2M amyloid fibrils. The intracellular B2M in monocytes/macrophages infiltrating the osteoarticular tissue may form amyloid fibrils, as well as activating the inflammasome, which also induces pyroptotic cell death and IL-1β secretion leading to further inflammation and amyloid deposition in the extracellular matrix. Thus, the intracellular formation of B2M amyloid fibrils may contribute to osteoarticular deposition of B2M amyloid fibrils and inflammation in patients with DRA.

Ethics approval

Ethical approval for this study was obtained from *by the Human Research Ethical Committees of Ehime University (APPROVAL NUMBER/ID1301001)

Informed consent

Written informed consent was obtained from all subjects before the study.

ORCID iD

Junya Masumoto https://orcid.org/0000-0003-0847-0456

References

1. Berggård I (1976) Beta2-Microglobulins: isolation, properties, and distribution. *Federation Proceedings* 35: 1167–1170.
2. Gejyo F, Homma N, Suzuki Y, et al. (1986) Serum levels of β2-Microglobulin as a new form of amyloid protein in patients undergoing long-term hemodialysis. *New England Journal of Medicine* 314: 585–586. DOI: 10.1056/NEJM198602273140920
3. Naiki H, Higuchi K, Nakakuki K, et al. (1991) Kinetic analysis of amyloid fibril polymerization in vitro. *Laboratory investigation; a journal of technical methods and pathology* 65: 104–110.
4. Campistol JM, Torras A and Lopez-Pedret J (1988) Systemic character and visceral involvement of dialysis amyloidosis. *Clinical nephrology* 29: 105–106.
5. Schiffl H (2014) Impact of advanced dialysis technology on the prevalence of dialysis-related amyloidosis in long-term maintenance dialysis patients. *Hemodialysis international* 18: 136–141. DOI: 10.1111/hdi.12057
6. Nishi S, Hoshino J, Yamamoto S, et al. (2018) Multicentre cross-sectional study for bone-articular lesions associated with dialysis related amyloidosis in Japan. *Nephrology* 23: 640–645. DOI: 10.1111/nep.13077
7. Portales-Castillo I, Yee J, Tanaka H, et al. (2020) Beta-2 Microglobulin amyloidosis: past, present, and future. *Kidney* 1: 1447–1455. DOI: 10.34067/KID.0004922020
8. Merlini G and Bellotti V (2003) Molecular mechanisms of amyloidosis. *New England Journal of Medicine* 349: 583–596. DOI: 10.1056/NEJMra023144
9. Gejyo F, Yamada T, Odani S, et al. (1985) A new form of amyloid protein associated with chronic hemodialysis was identified as β2-microglobulin. *Biochemical and Biophysical Research Communications* 129: 701–706. DOI: 10.1016/0006-291x(85)91948-91945
10. Kaneko S and Yamagata K (2018) Hemodialysis-related amyloidosis: Is it still relevant? *Seminars in Dialysis* 31: 612–618. DOI: 10.1111/sdi.12720
11. Yamamoto S, Kazama JJ, Maruyama H, et al. (2013) Dialysis-related amyloidosis: pathogenesis and clinical features in patients undergoing dialysis treatment. In: Feng D (ed) *Amyloidosis*. London: IntechOpen, pp. 67–83.
12. Naiki H, Hashimoto N, Suzuki S, et al. (1997) Establishment of a kinetic model of dialysis-related amyloid fibril extensionin vitro. *Amyloid* 4: 223–232. DOI: 10.3109/13506129709003833
13. Zhang P, Fu X, Sawashita J, et al. (2010) Mouse model to study human A β2M amyloidosis: generation of a transgenic mouse with excessive expression of human β2-microglobulin. *Amyloid* 17: 50–62. DOI: 10.3109/13506129.2010.483116
14. Luger A, Kovarik J, Stummvoll HK, et al. (1987) Blood-membrane interaction in hemodialysis leads to increased cytokine production. *Kidney International* 32: 84–88. DOI: 10.1038/ki.1987.175
15. Kimmel PL, Phillips TM, Phillips E, et al. (1990) Effect of renal replacement therapy on cellular cytokine production in patients with renal disease. *Kidney International* 38: 129–135. DOI: 10.1038/ki.1990.177
16. Halle A, Hornung V, Petzold GC, et al. (2008) The NALP3 inflammasome is involved in the innate immune response to amyloid-β. *Nature Immunology* 9: 857–865. DOI: 10.1038/ni.1636
17. Masters SL, Dunne A, Subramanian SL, et al. (2010) Activation of the NLRP3 inflammasome by islet amyloid

polypeptide provides a mechanism for enhanced IL-1β in type 2 diabetes. *Nature Immunology* 11: 897–904. DOI: 10.1038/ni.1935

18. Niemi K, Teirilä L, Lappalainen J, et al. (2011) Serum amyloid A activates the NLRP3 inflammasome via P2X7 receptor and a cathepsin B-sensitive pathway. *The Journal of Immunology* 186: 6119–6128. DOI: 10.4049/jimmunol.1002843

19. Ather JL, Ckless K, Martin R, et al. (2011) Serum amyloid A activates the NLRP3 inflammasome and promotes Th17 allergic asthma in mice. *The Journal of Immunology* 187: 64–73. DOI: 10.4049/jimmunol.1100500

20. Nakanishi A, Kaneko N, Takeda H, et al. (2018) Amyloid β directly interacts with NLRP3 to initiate inflammasome activation: identification of an intrinsic NLRP3 ligand in a cell-free system. *Inflammation and Regeneration* 38: 27. DOI: 10.1186/s41232-018-0085-6

21. Morikawa S, Kaneko N, Okumura C, et al. (2018) IAPP/amylin deposition, which is correlated with expressions of ASC and IL-1β in β-cells of Langerhans' islets, directly initiates NLRP3 inflammasome activation. *International Journal of Immunopathology and Pharmacology* 32: 205873841878874. DOI: 10.1177/2058738418788749

22. Mori W, Kaneko N, Nakanishi A, et al. (2021) Insulin amyloid fibrils interact directly with the NLRP3, resulting in inflammasome activation and pyroptotic cell death. *International Journal of Immunopathology and Pharmacology* 35: 205873842110383. DOI: 10.1177/20587384211038357

23. Hofbauer D, Mougiakakos D, Broggini L, et al. (2021) β2-microglobulin triggers NLRP3 inflammasome activation in tumor-associated macrophages to promote multiple myeloma progression. *Immunity* 54: 1772–1787. DOI: 10.1016/j.immuni.2021.07.002

24. Zako T, Sakono M, Kobayashi T, et al. (2012) Cell interaction study of amyloid by using luminescent conjugated polythiophene: implication that amyloid cytotoxicity is correlated with prolonged cellular binding. *ChemBioChem* 13: 358–363. DOI: 10.1002/cbic.201100467

25. Ohhashi Y, Hagihara Y, Kozhukh G, et al. (2002) The intrachain disulfide bond of 2-microglobulin is not essential for the immunoglobulin fold at neutral pH, but is essential for amyloid fibril formation at acidic pH. *Journal of Biochemistry* 131: 45–52. DOI: 10.1093/oxfordjournals.jbchem.a003076

26. Kaneko N, Ito Y, Iwasaki T, et al. (2017) Poly (I:C) and hyaluronic acid directly interact with NLRP3, resulting in the assembly of NLRP3 and ASC in a cell-free system. *European Journal of Inflammation* 15: 85–97. DOI: 10.1177/1721727X17711047

27. Sugiyama R, Agematsu K, Migita K, et al. (2014) Defect of suppression of inflammasome-independent interleukin-8 secretion from SW982 synovial sarcoma cells by familial Mediterranean fever-derived pyrin mutations. *Molecular*

Biology Reports 41: 545–553. DOI: 10.1007/s11033-013-2890-y

28. Masumoto J, Taniguchi Si., Ayukawa K, et al. (1999) ASC, a novel 22-kDa protein, aggregates during apoptosis of human promyelocytic leukemia HL-60 cells. *Journal of biological chemistry* 274: 33835–33838. DOI: 10.1074/jbc.274.48.33835

29. Iwasaki T, Kaneko N, Ito Y, et al. (2016) Nod2-Nodosome in a cell-free system: implications in pathogenesis and drug discovery for blau syndrome and early-onset sarcoidosis. *TheScientificWorldJournal* 2016: 2597376. DOI: 10.1155/2016/2597376

30. Kaneko N, Kurata M, Yamamoto T, et al. (2020) KN3014, a piperidine-containing small compound, inhibits auto-secretion of IL-1β from PBMCs in a patient with Muckle-Wells syndrome. *Scientific Reports* 10: 13562. DOI: 10.1038/s41598-020-70513-0

31. Mokuda S, Kanno M, Takasugi K, et al. (2014) Tocilizumab improved clinical symptoms of a patient with systemic tophaceous gout who had symmetric polyarthritis and fever: an alternative treatment by blockade of interleukin-6 signaling. *SAGE open medical case reports* 2: 2050313X1351977. DOI: 10.1177/2050313X13519774

32. Kihara M, Chatani E, Sakai M, et al. (2005) Seeding-dependent maturation of β2-microglobulin amyloid fibrils at neutral pH. *Journal of biological chemistry* 280: 12012–12018. DOI: 10.1074/jbc.M411949200

33. Zhou W, Kaneko N, Nakagita T, et al. (2021) A comprehensive interaction study provides a potential domain interaction network of human death domain superfamily proteins. *Cell Death & Differentiation* 28: 2991–3008. DOI: 10.1038/s41418-021-00796-x

34. Naiki H, Okoshi T, Ozawa D, et al. (2016) Molecular pathogenesis of human amyloidosis: lessons from β2-microglobulin-related amyloidosis. *Pathology International* 66: 193–201. DOI: 10.1111/pin.12394

35. Naiki H, Hashimoto N, Suzuki S, et al. (1997) Establishment of a kinetic model of dialysis-related amyloid fibril extensionin vitro. *Amyloid* 4: 223–232.

36. Yamamoto S, Kazama JJ, Narita I, et al. (2009) Recent progress in understanding dialysis-related amyloidosis. *Bone* 45(suppl 1): S39–S42. DOI: 10.1016/j.bone.2009.03.655

37. Yamamoto S, Yamaguchi I, Hasegawa K, et al. (2004) Glycosaminoglycans enhance the trifluoroethanol-induced extension of 2-microglobulin-related amyloid fibrils at a neutral pH. *Journal of the American Society of Nephrology* 15: 126–133. DOI: 10.1097/01.asn.0000103228.81623.c7

38. Bjerrum OW, Bjerrum OJ and Borregaard N (1987) Beta 2-microglobulin in neutrophils: an intragranular protein. *Journal of immunology* 138: 3913–3917.

39. Stone PJ, Campistol JM, Abraham CR, et al. (1993) Neutrophil proteases associated with amyloid fibrils. *Biochemical and Biophysical Research Communications* 197: 130–136. DOI: 10.1006/bbrc.1993.2451

40. Mansfield E, Chae JJ, Komarow HD, et al. (2001) The familial Mediterranean fever protein, pyrin, associates with microtubules and colocalizes with actin filaments. *Blood* 98: 851–859. DOI: 10.1182/blood.v98.3.851

41. Hu J, Han J, Li H, et al. (2018) Human embryonic kidney 293 cells: a vehicle for biopharmaceutical manufacturing, structural biology, and electrophysiology. *Cells Tissues Organs* 205: 1–8. DOI: 10.1159/000485501

42. Compan V and López-Castejón G (2016) Functional reconstruction of NLRs in HEK293 cells. *Methods in Molecular Biology* 1417: 217–221. DOI: 10.1007/978-1-4939-3566-6_15

43. Shi H, Murray A and Beutler B (2016) Reconstruction of the mouse inflammasome system in HEK293T cells. *Bio-protocol* 6: e1986. DOI: 10.21769/BioProtoc.1986

44. Noji M, Sasahara K, Yamaguchi K, et al. (2019) Heating during agitation of β2-microglobulin reveals that supersaturation breakdown is required for amyloid fibril formation at neutral pH. *Journal of Biological Chemistry* 294: 15826–15835. DOI: 10.1074/jbc.RA119.009971

45. Noji M, Samejima T, Yamaguchi K, et al. (2021) Breakdown of supersaturation barrier links protein folding to amyloid formation. *Communications Biology* 4: 120. DOI: 10.1038/s42003-020-01641-6

46. Balci-Peynircioglu B, Waite AL, Schaner P, et al. (2008) Expression of ASC in renal tissues of familial Mediterranean fever patients with amyloidosis: postulating a role for ASC in AA type amyloid deposition. *Experimental Biology and Medicine* 233: 1324–1333. DOI: 10.3181/0803-RM-106